Original article

Nuclear Medicine Communications

Impact of image processing in the detection of ischaemia using CZT-SPECT/CT

Daniëlle Koopman[a], Jorn A. van Dalen[b], Cornelis H. Slump[a], Dimitri Lots[d], Jorik R. Timmer[c] and Pieter L. Jager[d]

Background **The new multipinhole cardiac single photon emission computed tomography/computed tomography (SPECT/CT) cameras with cadmium–zinc–telluride (CZT) detectors are highly sensitive and produce images of high quality but rely on complex dedicated reconstruction algorithms. The aim of this study was to determine the impact of various processing steps on image formation and in the detection of ischaemia in CZT-SPECT/CT both with and without attenuation correction (AC).**

Materials and methods **Data on 20 consecutive patients who underwent a 1-day protocol stress–rest SPECT/CT using ^{99m}Tc-tetrofosmin were processed twice by three experienced operators, yielding 120 AC and 120 noncorrected (NC) data sets. Processing steps included selection and determination of myocardial axes, manual SPECT/CT coregistration for AC and myocardial masking. Using the 17-segment cardiac model, differences between stress and rest segmental uptake (%) were calculated for NC and AC image sets. Both interoperator and intraoperator variations were considered significant for the diagnosis of ischaemia when greater than 5%.**

Results **The mean interoperator variations were 2.4 ± 1.4% (NC) and 3.8 ± 1.9% (AC) ($P < 0.01$). In 6% (NC) and 23% (AC) of the 120 processed cases, operator variation was larger than 5% and therefore potentially clinically interfering with the diagnosis of ischaemia. Differences between interoperator and intraoperator variations were nonsignificant.**

Conclusion **Operator variations in the processing of myocardial perfusion image data using CZT-SPECT/CT are significant and may influence the diagnosis of ischaemia, especially when AC is applied. Clearer guidelines for image processing are necessary to improve the reproducibility of the studies and to obtain a more reliable diagnosis of ischaemia.** ***Nucl Med Commun*** **36:60–68 © 2014 Wolters Kluwer Health | Lippincott Williams & Wilkins.**

Nuclear Medicine Communications 2015, **36**:60–68

Keywords: attenuation and scatter correction, image processing, misregistrations, myocardial ischaemia, myocardial perfusion imaging, single photon emission computed tomography

[a]MIRA Institute for Biomedical and Technical Medicine, University of Twente, Enschede, Departments of [b]Medical Physics, [c]Cardiology and [d]Nuclear Medicine, Isala Hospital, Zwolle, The Netherlands

Correspondence to Daniëlle Koopman, BSc, Department of Nuclear Medicine, Isala Hospital, Dokter van Heesweg 2, 8025 AB Zwolle, The Netherlands
Tel: +31 384 245238; fax: +31 384 247604; e-mail: d.koopman@isala.nl

Received 8 April 2014 **Revised** 30 May 2014 **Accepted** 3 August 2014

Introduction

Myocardial perfusion scintigraphy (MPS) with single photon emission computed tomography (SPECT) cameras is widely used as a noninvasive imaging modality for the detection of ischaemia [1]. Conventional SPECT cameras, using sodium iodide technology, have been proven to provide valuable diagnostic and prognostic information [2–4]. With the use of the iterative reconstruction algorithm ordered subset expectation maximization with incorporated collimator detector response modelling as well as attenuation correction (AC) and scatter correction, image resolution was further increased [5]. Furthermore, several studies have shown that the addition of AC by computed tomography (CT) to MPS increases the certainty of interpretation [6–8], although some controversy remains [9–11]. A limitation in the use of CT-based AC is that emission (SPECT) and subsequent transmission (CT) take place sequentially. This allows the possibility of patient motion between the two acquisitions, resulting in misregistration [12]. Such misregistrations may be present in up to 40% of cases [13,14]. Misregistrations increase the likelihood of artefactual perfusion defects [15,16], resulting in decreased sensitivity and specificity [17].

With the introduction of the new multipinhole dedicated cardiac SPECT/CT cameras with cadmium zinc telluride (CZT) detectors, the higher-energy resolution and count sensitivity lead to improved image quality and interpretation of MPS [18,19]. In addition, for CZT pixel detectors, Montemont *et al.* [20] showed that the new focused collimator CZT-detector design in combination with ordered subset expectation maximization further improves the image resolution. Because of these improvements, manual image processing may significantly impact SPECT image formation and thereby image interpretation.

A part of the data described in this manuscript were presented at the 11th International Conference of Noninvasive Cardiovascular Imaging (ICNC) and published as an abstract in a Supplement of the *Journal of Nuclear Cardiology*, volume 20 in May/June 2013. Data were also partly presented during an oral presentation at the European Association of Nuclear Medicine (EANM) 2013, Lyon.

0143-3636 © 2014 Wolters Kluwer Health | Lippincott Williams & Wilkins

DOI: 10.1097/MNM.0000000000000200

Image processing consists of four manual steps: selection of the myocardium, determination of myocardial axes and boundaries, SPECT/CT coregistration and masking of the myocardium. The effect of misalignment of CT and SPECT on image interpretation has been well described for conventional cameras using sodium iodide technology [12–17]. However, the particular influence of CZT-based SPECT/CT systems is as yet unknown. Moreover, the influence of the other three manual steps on the SPECT image formation and interpretation has not been determined previously. It is expected that operator variations in these steps influence stress and/or rest data. Hence, this can influence the comparison between stress and rest studies and consequently the diagnosis of ischaemia.

Therefore, the aim of this study was to determine the impact of various processing steps in CZT-based SPECT, including the effect of AC, in the detection of ischaemia. For this purpose we have determined the effect of operator variability of the processing steps on the final outcome of MPS studies.

Materials and methods

Study population

Twenty consecutive patients who underwent stress and rest SPECT/CT imaging were included after written informed consent was obtained. Patient characteristics, including sex, age and BMI were collected for analysis.

Patient preparation

Patients underwent a 1-day ^{99m}Tc-tetrofosmin stress and rest examination. By means of intravenous administration of adenosine, pharmacological stress was induced. The dose in the stress study was 370 MBq for patients with a body weight up to 100 kg and 500 MBq for patients with a body weight above 100 kg. The rest injected dose was 740 MBq for patients weighing up to 100 kg and 1000 MBq for patients greater than 100 kg. To prevent the influence of the remaining stress activity during acquisition of the rest study, a time interval of at least 3 h was maintained between stress and rest data acquisition.

SPECT/CT data acquisition

All patients were scanned with a CZT-based SPECT/CT camera (Discovery NM/CT 570c; GE Healthcare, Fairfield, Connecticut, USA). Stress and rest SPECT images were acquired 45–60 min after tracer injection. Acquisition times for stress and rest imaging were 5 and 4 min, respectively. Data were acquired using a multi-pinhole camera, which contains 19 stationary CZT detectors simultaneously imaging the heart. Each detector contains 32×32 pixelated (2.46×2.46 mm) CZT elements. A symmetrical 20% wide energy window at 140.5 keV was used. Stress and rest SPECT images were reconstructed using a maximum-likelihood expectation maximization reconstruction algorithm. SPECT image voxel size was $4 \times 4 \times 4$ mm^3.

For optimal image quality in terms of detecting perfusion defects and uniformity of normal myocardium, all reconstruction parameters were set to default values supplied by the manufacturer. Noncorrected (NC) and AC data (for both stress and rest studies) were reconstructed with 30 and 60 iterations, respectively. Postfiltering was applied using a three-dimensional Butterworth filter with a cutoff frequency of 0.40 cycle/cm and power 10 for NC data, whereas for AC data these parameters were 0.37 and 7, respectively. No scatter correction was applied, as this was not incorporated in the manufacturer's default settings.

Both stress and rest SPECT studies were followed by a low-dose 64-slice CT during breath-hold (after expiration) to provide an attenuation map. Helical CT scans were acquired using 120 kV, a tube current of 20 mA and 800 ms rotation time. CT images were reconstructed using filtered back projection with a 512×512 matrix, a pixel size of 1×1 mm^2 and a slice thickness of 5.0 mm. Both SPECT and CT data were processed using a dedicated reconstruction algorithm available in a Xeleris Workstation (GE Healthcare). This algorithm translates the raw data of the 19 pinhole detectors into a three-dimensional matrix, correcting for position and angulations of the detectors. It inherently contains image distortion outside the central field of view (containing the myocardium) for which the system has been optimized.

Image processing

The SPECT/CT data were processed twice by three experienced operators. Between the first and second processing session for each patient, a time period of at least 1 week was applied to minimize memory effects. In addition, the images were selected randomly in both sessions. In the order of execution, the processing steps included selection of the myocardium, determination of myocardial axes and boundaries, manual SPECT/CT coregistration for AC and masking of the myocardial surrounding. Coregistration between SPECT and CT data sets was performed by means of rigid transformation with six degrees of freedom: translation and rotation in three directions. All processing steps were performed separately for stress and rest studies. For each SPECT image, normalization of maximum peak activity to 100% was performed automatically. After the data of a patient were processed, two screen captures containing the stress and rest 17-segment polar maps of the left ventricle (for both NC and AC data) were saved. For each segment, the tracer uptake was calculated as the percentage of the maximum left ventricular uptake [21]. Measurements of the ejection fraction (EF) and end-diastolic volume (EDV) were also saved for analysis.

Data analysis

As three operators processed the stress and rest SPECT/CT data twice for all 20 patients (both NC and

AC), 240 NC and 240 AC data sets were obtained. For each segment of each particular data set, the difference between the stress and rest perfusion value (SRD) was calculated. The resulting 120 NC and 120 AC data sets were subsequently used to define segment-based and patient-based variation. Afterwards, interoperator, intraoperator, segment-based and perfusion-based analyses were performed.

Definition segment-based variation

When comparing two SRD data sets (derived either by two operators or by one operator who processed the data twice) segment by segment, the processing variation was determined by calculating the absolute difference in SRD for each segment between two data sets. This variation is called segment-based variation. Use of the absolute difference in SRD implies that the processing variations are always positive.

Definition patient-based variation

Two SRD data sets of a single patient were compared by calculating the average segment-based variation across all 17 segments. This variation is called patient-based variation.

Interoperator analysis

For interoperator analysis, the results obtained by the three operators who processed the data sets of 20 patients twice were compared using patient-based variation. For each of the three independent combinations of operators, results of both processing sessions were compared. This resulted in six interoperator comparisons for the SRD data sets. The mean interoperator variation across the six sets was determined as the average of the six interoperator comparisons.

Intraoperator analysis

For intraoperator analysis, the SRD data sets resulting from both processing sessions of the three operators were compared for the 20 patients separately by calculating the patient-based variation. The results were averaged across all patients and the three operators to determine the mean intraoperator variations.

Segment-based analysis

Using the interoperator data in terms of segment-based variation, a segment-based analysis was performed. For each segment (1–17), the mean variations of the six interoperator comparisons were determined. Subsequently, the mean variations of the outer segments 1–6 and the inner segments 7–17 were compared.

Perfusion-based analysis

After determining the patient-based interoperator variations, correlations with myocardial perfusion, patient's BMI, EDV and EF of the left ventricle were analysed. MPS scans were evaluated by teams of experienced cardiologists and nuclear medicine physicians. Segments were scored semiquantitatively by consensus of two readers using the 17-segment model with the following five-point scoring system: 0 = normal, 1 = equivocal radiotracer uptake, 2 = moderate reduction in radiotracer uptake, 3 = severe reduction in radiotracer uptake and 4 = absence of detectable tracer in a segment. Perfusion defects were identified on the stress images, in which a segment with a score of at least 2 was considered to have a defect. A reversible perfusion defect was defined as one in which a stress defect was associated with a rest score of 1 or less or a stress defect score of 4 with a rest score of 2 or less. When a perfusion defect on the stress images was not associated with increased perfusion on rest images (rest score > 2), the defect was defined as irreversible [19]. For myocardial perfusion analysis, the patients were divided into two groups. The first group comprised all patients with a normal MPS study, and the second group comprised all patients with myocardial perfusion defects. In this way all perfusion defects were included in the second group, such as mild and severe ischaemia and reversible and irreversible defects.

Data interpretation

With respect to quantitative analysis, an SRD between 5 and 9% was considered as mild ischaemia. A stress–rest difference of at least 10% was defined as moderate to severe ischaemia [22]. Differences between mild and moderate to severe ischaemia may have significant clinical impact, as mild ischaemia justifies an expectative policy and moderate to severe ischaemia may be further analysed using angiography [23]. For segment-based analysis, processing variation was considered significant for the diagnosis of ischaemia if larger than 5% in at least two segments. In this perspective we determined the number of patients having more than 5 and 10% processing variation in at least two segments for each interoperator set. For patient-based analysis, processing variation was considered significant when the average was larger than 5%. Therefore, the number of patients with more than 5% patient-based processing variation was determined from the 120 patient-based interoperator comparisons.

Causes and consequences of operator variation

An additional analysis of the causes and consequences of the resulting variations was performed. The aim of image coregistration was to accurately superimpose the cardiac attenuation data from the CT scan to the cardiac radiotracer activity data from the SPECT scan [21]. The gold standard for SPECT/CT coregistration was defined as a visually assessed full overlap on the transaxial sections between SPECT and CT myocardium, without SPECT myocardium located in CT lung tissue or in ventrally located fat tissue. In that perspective, a misregistration was defined as a mismatch of at least 3 mm on any transaxial section between SPECT and CT myocardium.

Mismatches were visually assessed and measured using Xeleris software (GE Healthcare). For patient-based AC variations larger than 5%, the number of misregistrations between SPECT and CT was determined. In a subanalysis, we analysed how the processing steps of selection and masking of the myocardium contributed to the 17-segment values. Two forms of selection (broad and small) and two forms of masking (no masking vs. masking) were applied on the stress scans of eight out of the 20 patients, without varying the other variables like coregistration of the SPECT/CT data or orienting the myocardial axes. The resulting 17-segment cardiac models were analysed.

Statistical analysis

Quantitative perfusion data were presented as mean ± SD. Categorical variables were presented as mean or percentages. The comparison method consisted of a segment-dependent, patient-dependent and operator-dependent analysis to differentiate between segment-based, patient-based and operator-based variation. Student's *t*-test was used to compare the patient-based operator variation between AC and NC studies, outer versus inner segments and normal versus abnormal myocardial perfusion function. Agreement among the three operators was evaluated by means of analysis of variance. Linear regression analysis was used to determine regression coefficients between patient-based interoperator variation and BMI, EDV and EF. A *P*-value less than 0.05 was considered statistically significant. Statistical analysis was performed using Microsoft Office Excel 2007 software (Microsoft, Redmond, Washington, USA).

Results

The study population consisted of seven women and 13 men (age: 34–79 years; BMI: 21.8–39.6 kg/m^2; EDV: 50.0–183.0 ml; and EF: 52.0–78.0%). A total of 8160 segments (20 patients × 17 segments × 3 operators × 2 processing sessions × 2 'AC and NC data' × 2 'stress and rest study') were evaluated in this study. In Fig. 1 an illustration of the selection of the processing steps, determination of myocardial axes and boundaries and masking of the myocardium is presented. Figure 2 shows an example of SPECT/CT coregistration, in accordance with the gold standard.

Interoperator and intraoperator variation

In Fig. 3 the interoperator variations per patient for processing session 1 (sets 1, 3 and 5) are presented. There was a large range in processing variation between operators and patients for NC and AC data sets. In Table 1 the mean interoperator and intraoperator variations and the range between the 20 patients are presented for NC and AC data sets. The mean interoperator variations across the six interoperator sets were 2.4 ± 1.4% for NC and 3.8 ± 1.9% for AC data sets ($P < 0.01$). Manual AC increased the mean operator variation by a factor of 1.6. The differences between the six interoperator sets were nonsignificant ($P = 0.46$ for NC data and $P = 0.08$ for AC data). With respect to the intraoperator variations, differences between NC and AC data sets were significant ($P < 0.01$), whereas differences between the two sessions of one operator were nonsignificant ($P = 0.45$ for NC data and $P = 0.07$ for AC data). Interoperator variations were not significantly different from intraoperator variations ($P = 0.32$ for NC data and $P = 0.07$ for AC data).

Patient-based variation larger than 5%

In 5.8% (seven out of 120 cases: 20 patients × 6 interoperator comparisons), the mean NC variation was larger than 5%. In 22.5% (27 out of 120 cases), the variation was larger than 5% for AC data sets.

Segments 1–6 versus segments 7–17

Figure 4 visualizes the mean segment-based variation for each of the 17 segments of the cardiac model. The mean segment-based variations of the outer segments 1–6, calculated across all patients and operators, were 3.7 ± 3.0% (NC) and 6.0 ± 4.7% (AC). For the inner segments 7–17, these variations were 1.7 ± 1.6 and 2.7 ± 2.3%, respectively. In other words, the variation in the outer segments 1–6 was 2.2 times larger than the variation in the inner segments, which was statistically significant ($P < 0.01$). In Fig. 5 an example of a stress–rest AC study processed by two operators has been presented, in which diagnosis of ischaemia has been compromised. In this study, a perfusion defect is present in segments 9, 10 and 15. For one operator (Fig. 5a and c) the maximum SRD is 8% in this region, which represents mild ischaemia. However, for the other operator (Fig. 5b and d), the SRD differences increased up to 10–15%, representing moderate to severe ischaemia. Table 2 shows the number and percentage of patient studies that contained more than 5 and 10% variation in at least two segments for the six interoperator NC and AC data sets.

Perfusion analysis

NC and AC mean interoperator variations for the subgroup of patients with normal perfusion were 2.2 ± 0.5 and 3.8 ± 1.4%, respectively. In the subgroup of patients with a perfusion defect, NC and AC interoperator variations were 2.5 ± 1.2 and 3.9 ± 1.0%, respectively. Differences between these subgroups were nonsignificant for both NC and AC interoperator variations ($P = 0.39$ and 0.23, respectively). Between BMI and mean NC interoperator variation, a significant correlation ($P = 0.02$) was found with a regression coefficient of 0.50. No significant correlation was found between BMI and mean AC interoperator variation ($P = 0.51$). The regression coefficient was 0.15. In Fig. 6 the relation between the mean interoperator variation and BMI is presented in a scatter plot. With respect to EDV and EF, no significant correlations for NC and AC interoperator variations were

Fig. 1

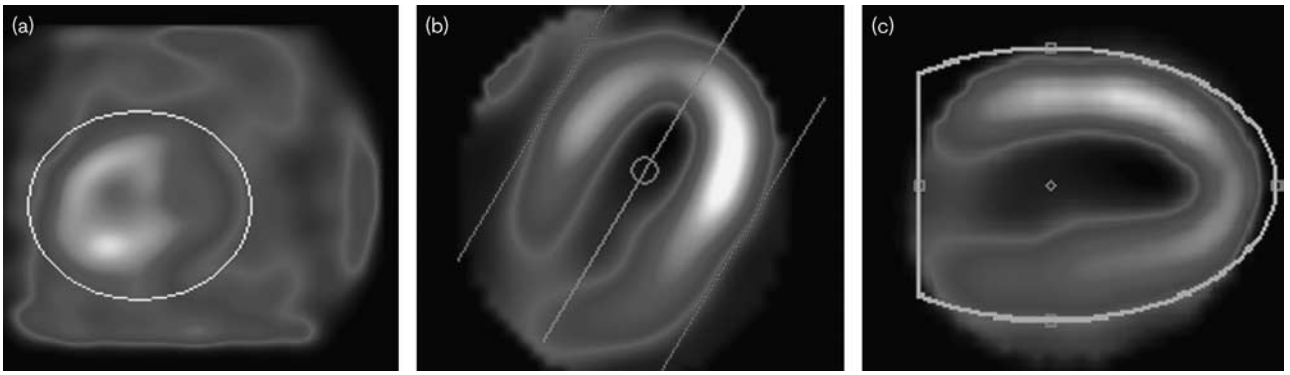

Visualization of the processing steps: selection (a), determination of myocardial axes and boundaries (b) and masking of the myocardium (c).

Fig. 2

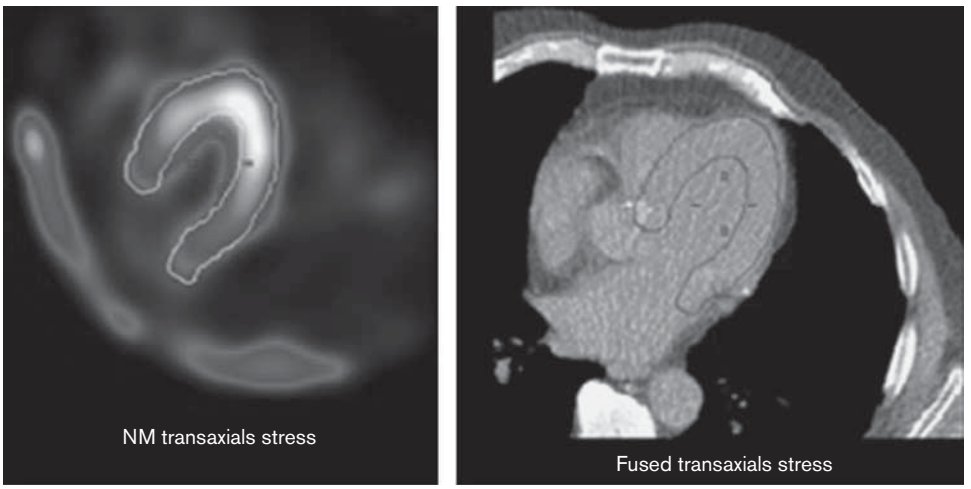

Example of the coregistration between SPECT and CT myocardium in the transaxial section, in accordance with the gold standard for coregistration. CT, computed tomography; SPECT, single photon emission computed tomography.

found. For the EDV, the *P*-values for NC and AC variations were 0.40 and 0.56 with regression coefficients of 0.21 and 0.14, respectively. For the EF, the NC and AC regression coefficients were 0.01 and 0.45 with *P*-values of 0.97 and 0.06, respectively.

Influence of different processing steps

SPECT/CT misregistrations

In all 27 cases (out of 120 cases) with a mean AC variation larger than 5%, a misregistration between SPECT and CT in the stress and/or rest data set was found. Misregistrations were mainly present in the ventral/dorsal or septal/lateral direction. In 15 out of the 27 misregistration cases (55.5%), misregistration between SPECT and CT occurred because it was impossible to align SPECT with CT with an absolute translation less than 3 mm.

Influence of selection and masking

The variation in the outer segments was significantly larger than the variation in the inner segments for both NC and AC data sets. Analysis showed that the influence of masking on the 17-segment values was small. Mean differences were $0.3 \pm 0.3\%$ (NC) and $0.9 \pm 0.9\%$ (AC) across eight patients and 17 segments. Mean differences between broad and small selection were $1.8 \pm 3.3\%$ (NC) and $3.3 \pm 3.1\%$ (AC). These differences were significant for both NC ($P = 0.04$) and AC data ($P < 0.01$). When a small selection was applied, the extra cardiac activity was already removed. This resulted in a polar map with less extra cardiac background, compared with the polar map after broad selection. Although the masking variation was not influenced by SPECT/CT coregistration, the influence of masking for AC data was significantly higher compared with that for NC data ($P < 0.01$). The influence

Fig. 3

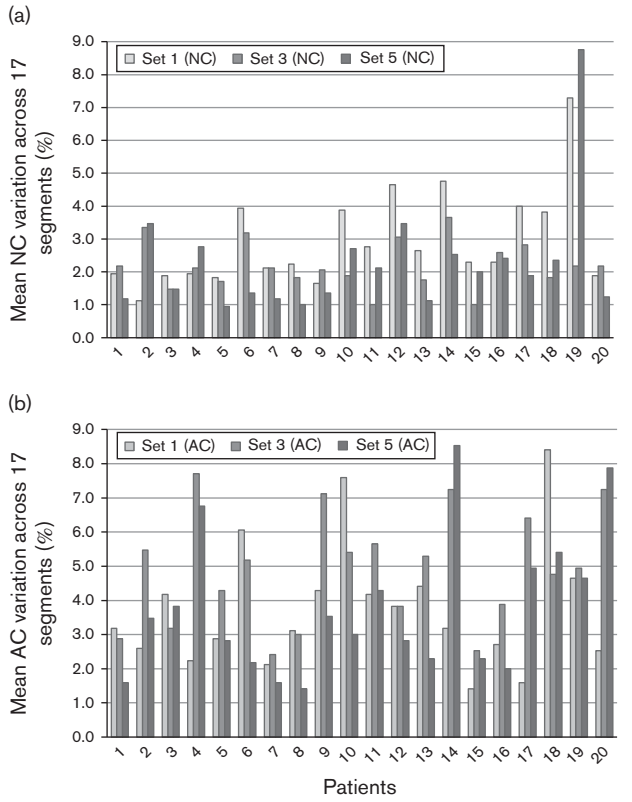

The amount of interoperator variation per patient for the (a) NC and (b) AC data sets for three interoperator sets (sets 1, 3 and 5) corresponding to processing session 1. The interoperator variation is the mean percentage difference between the stress and rest left ventricular uptake, for both NC and AC data sets, for each patient processed by two operators. AC, attenuation corrected; NC, noncorrected.

Table 1 The intraoperator and interoperator variations (mean ± SD) and the range between the 20 patients for noncorrected and attenuation-corrected data sets

	NC variation (%)	Range NC (%)	AC variation (%)	Range AC (%)
Interoperator variation				
Set 1	3.0 ± 1.5	1.1–7.3	3.8 ± 1.8	1.4–8.4
Set 2	2.5 ± 1.7	0.9–7.7	3.7 ± 1.8	1.1–7.5
Set 3	2.2 ± 0.7	1.0–3.7	4.9 ± 1.7	2.4–7.7
Set 4	2.2 ± 1.2	0.9–5.6	3.8 ± 2.3	1.7–11.2
Set 5	2.2 ± 1.7	0.9–8.8	3.8 ± 2.1	1.4–8.5
Set 6	2.2 ± 1.4	0.5–6.7	3.1 ± 1.4	1.0–6.9
Mean	2.4 ± 1.4		3.8 ± 1.9	
Intraoperator variation				
Operator 1	2.7 ± 2.3	0.9–12.6	4.4 ± 3.8	1.7–15.2
Operator 2	1.9 ± 0.8	0.8–4.0	2.8 ± 1.1	1.1–5.5
Operator 3	2.2 ± 2.1	0.5–9.9	3.2 ± 1.7	1.1–7.8
Mean	2.2 ± 1.7		3.5 ± 2.2	

Sets 1, 3 and 5 correspond to processing session 1; sets 2, 4 and 6 correspond to processing session 2.
Differences between NC and AC variations were significant for intraoperator and interoperator data sets.
Differences between operators and between two sessions of one operator were nonsignificant.
AC, attenuation corrected; NC, noncorrected.

Fig. 4

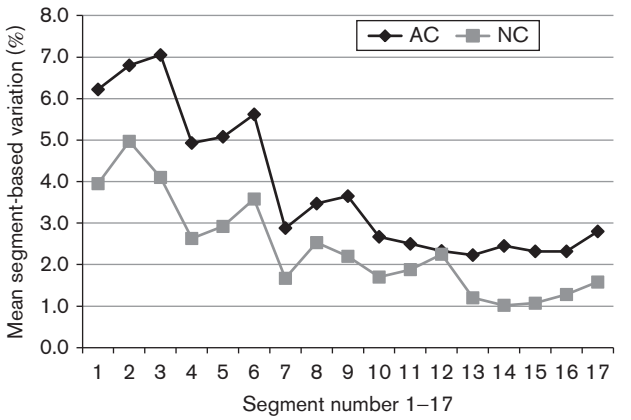

The mean interoperator variation for NC and AC data sets as a function of the 17 segments of the cardiac model. AC, attenuation corrected; NC, noncorrected.

of selection for AC data was similar compared with NC data ($P = 0.10$).

Discussion

In this study, we demonstrated that the stress–rest perfusion difference in CZT-SPECT may easily reach clinically relevant levels of 10% segmental perfusion only because of variation in processing. In particular, we found that intraoperator and interoperator variability was significantly larger for AC data sets compared with NC data sets. We showed that misregistrations significantly increased the AC operator variation. In 22.5% of our patients a mean AC variation of at least 5% was found. This indicates that the mild ischaemia range (5–9%) should be used with care as operator variation may induce or mask mild ischaemia. In other words, AC operator variation may upstage or downstage the severity of ischaemia. Furthermore, in 25.0% of the patients at least 10% variation in two segments of the 17-segment model was found. This means that, in 25% of the MPS scans, diagnosis of ischaemia based on the AC data set can be hampered because of image processing. Manual coregistration of SPECT and CT, needed for AC, increased the operator variation typically by 50%. We found intraoperator and interoperator variations to be similar, suggesting that processing errors are intrinsic.

As it is not possible to coregister stress and rest data with the processing software provided by the manufacturer, differences in myocardium selection and masking were likely to occur between stress and rest studies. This may influence SRD values and thereby mimic or mask perfusion defects. Therefore, it is recommended that operators should work in a similar manner to minimize processing-related discrepancies between stress and rest studies.

Fig. 5

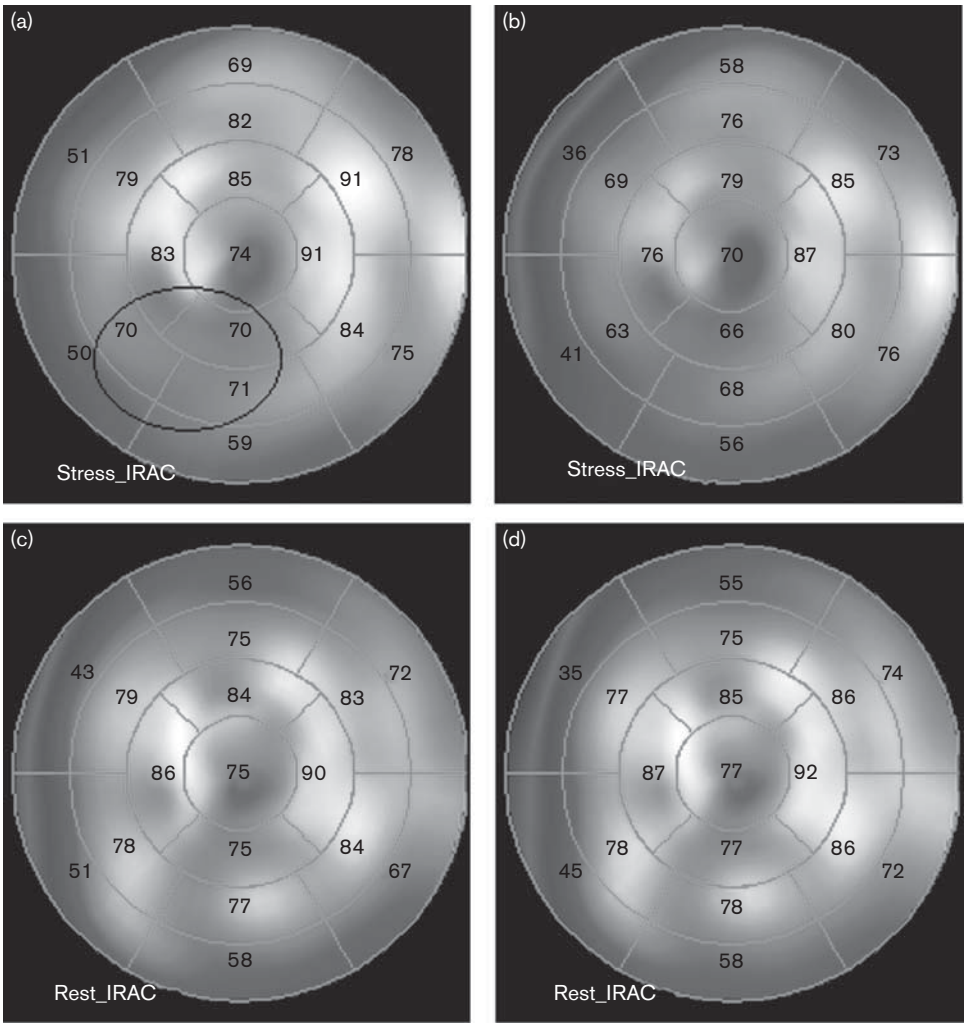

Example of a stress–rest AC study processed by operator 2 (a and c) and operator 3 (b and d) in which the operator variation may influence the diagnosis of ischaemia. On comparing the stress and rest SPECT images, a perfusion defect was detected in the inferoseptal region (segments 9, 10 and 15, black circle). However, the severity of the defect differed for the two processed studies. When evaluating the left data set, the perfusion defect was regarded as mild ischaemia with SRD perfusion values of 5–8%. However, when the right data set was used for clinical evaluation, the perfusion defect was regarded as moderate to severe ischaemia with SRD perfusion values of at least 10% for segments 9, 10 and 15. AC, attenuation corrected; SPECT, single photon emission computed tomography; SRD, stress and rest perfusion value difference.

Table 2 The number and percentage of patients in noncorrected and attenuation-corrected data sets of six interoperator sets that contained more than 5 and 10% variation in at least two segments

Interoperator sets ($n = 20$)	More than 5% NC variation in at least two segments [n (%)]	More than 5% AC variation in at least two segments [n (%)]	More than 10% NC variation in at least two segments [n (%)]	More than 10% AC variation in at least two segments [n (%)]
Set 1	11 (55.0)	15 (75.0)	1 (5.0)	5 (25.0)
Set 2	8 (40.0)	15 (75.0)	2 (10.0)	6 (30.0)
Set 3	6 (30.0	12 (60.0)	1 (5.0)	5 (25.0)
Set 4	7 (35.0)	10 (50.0)	2 (10.0)	1 (5.0)
Set 5	9 (45.0)	19 (95.0)	0 (0.0)	11 (55.0)
Set 6	8 (40.0)	14 (70.0)	2 (10.0)	4 (20.0)
Mean	8 (40.0)	13 (65.0)	1 (5.0)	5 (25.0)

AC, attenuation corrected; NC, noncorrected.

A large range in operator variation was found between patients, which was different between operators. When comparing subgroups of patients with and without perfusion defect(s), no significant differences were found. In addition, we classified groups by means of other criteria such as the absence or presence of reversible or irreversible defects, or

Fig. 6

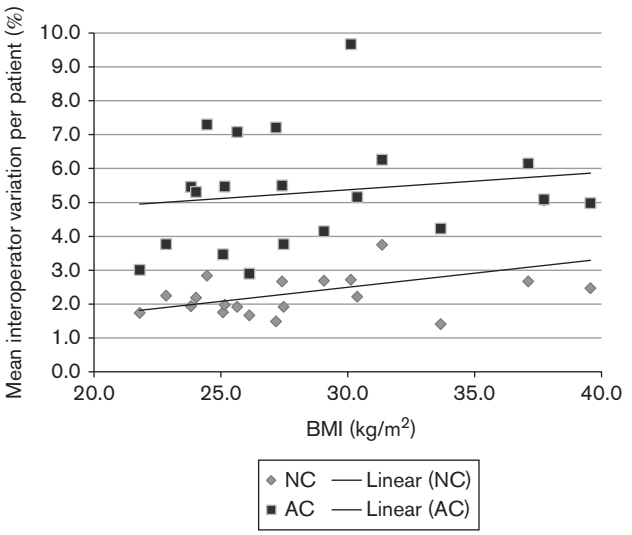

Scatter plot showing the relation between the mean interoperator variation per patient (NC and AC data sets) and patients' BMI. The correlation between mean NC interoperator variation and BMI was significant ($P = 0.02$) with a regression coefficient of 0.50. AC, attenuation corrected; NC, noncorrected.

the size of defects, but the mean variation differences between the groups remained nonsignificant. Further, patient characteristics such as EDV and EV do not explain this large range as they did not significantly influence the processing variation. Only BMI was significantly associated with an increased operator variation, but only when SPECT data were not corrected for attenuation. A possible reason is that image quality of NC SPECT images may decrease with increasing BMI because of increasing photon attenuation. Subsequently, this may have resulted in larger operator variations.

We showed that the outer segments of the 17-segment model are more sensitive for image processing compared with the inner segments for both NC and AC data sets. With respect to AC data sets, inaccurate coregistration of SPECT and CT images can cause artefacts especially in the outer segments. When we compared NC and AC data, we found significant difference in the influence of masking. This is possibly caused by differences in normalizations of NC and AC data. Moreover, selection of the myocardium significantly influenced the variation of myocardial perfusion in the outer segments. Broad selection includes greater extra cardiac activity, whereas small selection creates a greater magnified view of the myocardium without the presence of this activity. Therefore, we recommend consistent application of small selection of the myocardium.

More studies have focused on operator-induced variation and misregistration in myocardial SPECT imaging. Goetze *et al.* [13,14] showed quantitatively that misregistration of CT and SPECT frequently occurs in MPS. Our results with respect to SPECT/CT misregistrations are comparable to those of Kennedy *et al.* [17], who found clinically significant misregistrations in 23% of cases using conventional SPECT/CT. In their study, misregistrations along the ventral/dorsal axis most significantly affected AC myocardial perfusion image quality, whereas we mainly found mismatches in the ventral/dorsal and septal/lateral direction. In addition, we found that, in 55.5% of the misregistration cases, a perfect match between SPECT and CT images was impossible as the shape of the myocardium on the CT did not match the shape of the SPECT myocardium. This was probably due to patient movement during acquisition or due to our respiration protocol (expiration breath-hold during CT). The latter is supported by Gould *et al.* [24] who proved that acquiring a slow 29-s helical PET/CT scan during breathing resulted in significantly fewer artefactual myocardial defects due to misregistration compared with a fast 4-s helical PET/CT scan at end-expiratory breath-hold. We recommend that when SPECT/CT coregistrations cannot be performed satisfactorily the AC data set should be used with care. This conclusion is supported by the study of Kennedy *et al.* [17].

Another factor in the analysis of misregistration was based on our observation of operators at work. During SPECT/CT coregistration, both translation and rotation of the CT data can be used for matching. It appeared that the use of the rotation function varied considerably between operators, as in general operator 2 used the rotation function more often compared with operators 1 and 3. Although this did not result in significantly different operator variations, we recommend the use of the rotation function, as such rotations of the CT scan can clearly improve the myocardium coregistration with SPECT and thereby reduce misregistrations.

A potential drawback of this study is the mathematical method of analysis. We focused on quantitative analysis of the 17-segment model to assess processing variation, although visual interpretation of the 17-segment model and cardiac axes remain important in clinical practice. A gold standard was not available to test the diagnostic impact on our patient population on imaging using CZT-SPECT/CT. However, the 10% stress–rest difference that we used as a definition for the presence or absence of ischaemia is in agreement with commonly accepted values [22,25,26].

Finally, operator bias may have influenced the results. To minimize this, all operators processed the images twice for all 20 patients randomly and on different days. Although the participating operators knew the study perspective, they might have put extra effort into minimizing the variation, suggesting that in everyday practice the variation may be larger.

Conclusion

The impact of the various processing steps in MPS using CZT-based SPECT is significant. We found that intraoperator and interoperator variation may influence

the diagnosis of ischaemia in up to 25% of patients, especially when AC is applied. Operators should work in a similar manner, and departments should encourage efforts to reduce operator variation. Therefore, the strict use of quantitative myocardial perfusion data should be viewed with caution and requires knowledge of operator dependency. In particular, when a correct match between SPECT and CT is not possible, diagnosis should primarily be based on NC findings.

Taking these recommendations into account, a more stable image quality is expected, improving the detection of ischaemia in SPECT/CT studies and taking full advantage of the properties of CZT cameras.

Acknowledgements

Conflicts of interest

There are no conflicts of interest.

References

1 Hachamovitch R, Berman DS, Shaw LJ, Kiat H, Cohen I, Cabico JA, *et al.* Incremental prognostic value of myocardial perfusion single photon emission computed tomography for the prediction of cardiac death differential stratification for risk of cardiac death and myocardial infarction. *Circulation* 1998; **97**:535–543.

2 Beller GA, Zaret BL. Contributions of nuclear cardiology to diagnosis and prognosis of patients with coronary artery disease. *Circulation* 2000; **101**:1465–1478.

3 Shaw LJ, Iskandrian AE. Prognostic value of gated myocardial perfusion SPECT. *J Nucl Cardiol* 2004; **11**:171–185.

4 Marcassa C, Bax JJ, Bengel F, Hesse B, Petersen CL, Reyes E, Underwood R, European Council of Nuclear Cardiology (ECNC); European Society of Cardiology Working Group 5 (Nuclear Cardiology and Cardiac CT); European Association of Nuclear Medicine Cardiovascular. Clinical value, cost-effectiveness, and safety of myocardial perfusion scintigraphy: a position statement. *Eur Heart J* 2008; **29**:557–563.

5 Kovalski G, Keidar Z, Frenkel A, Israel O, Azhari H. Correction for respiration artefacts in myocardial perfusion SPECT is more effective when reconstructions supporting collimator detector response compensation are applied. *J Nucl Cardiol* 2009; **16**:949–955.

6 Hendel RC, Berman DS, Cullom SJ, Follansbee W, Heller GV, Kiat H, *et al.* Multicenter clinical trial to evaluate the efficacy of correction for photon attenuation and scatter in SPECT myocardial perfusion imaging. *Circulation* 1999; **99**:2742–2749.

7 Hendel RC, Corbett JR, Cullom SJ, DePuey EG, Garcia EV, Bateman TM. The value and practice of attenuation correction for myocardial perfusion SPECT imaging: a joint position statement from the American Society of Nuclear Cardiology and the Society of Nuclear Medicine. *J Nucl Med* 2002; **43**:273–280.

8 Thompson RC, Heller GV, Johnson LL, Case JA, Cullom SJ, Garcia EV, *et al.* Value of attenuation correction on ECG-gated SPECT myocardial perfusion imaging related to body mass index. *J Nucl Cardiol* 2005; **12**:195–202.

9 Watson DD. Is it time for SPECT attenuation correction? *J Nucl Cardiol* 2004; **11**:239–241.

10 Singh B, Bateman TM, Case JA, Heller G. Attenuation artifact, attenuation correction, and the future of myocardial perfusion SPECT. *J Nucl Cardiol* 2007; **14**:153–164.

11 Germano G, Slomka PJ, Berman DS. Attenuation correction in cardiac SPECT: the boy who cried wolf? *J Nucl Cardiol* 2007; **14**:25–35.

12 DePuey EG. Advances in SPECT camera software and hardware: currently available and new on the horizon. *J Nucl Cardiol* 2012; **19**:551–581.

13 Goetze S, Brown TL, Lavely WC, Zhang Z, Bengel FM. Attenuation correction in myocardial perfusion SPECT/CT: effects of misregistration and value of reregistration. *J Nucl Med* 2007; **48**:1090–1095.

14 Goetze S, Wahl RL. Prevalence of misregistration between SPECT and CT for attenuation-corrected myocardial perfusion SPECT. *J Nucl Cardiol* 2007; **14**:200–206.

15 Fricke H, Fricke E, Weise R, Kammeier A, Lindner O, Burchert W. A method to remove artifacts in attenuation-corrected myocardial perfusion SPECT introduced by misalignment between emission scan and CT-derived attenuation maps. *J Nucl Med* 2004; **45**:1619–1625.

16 Tonge CM, Manoharan M, Lawson RS, Shields RA, Prescott MC. Attenuation correction of myocardial SPECT studies using low resolution computed tomography images. *Nucl Med Commun* 2005; **26**:231–237.

17 Kennedy JA, Israel O, Frenkel A. Directions and magnitudes of misregistration of CT attenuation-corrected myocardial perfusion studies: incidence, impact on image quality, and guidance for reregistration. *J Nucl Med* 2009; **50**:1471–1478.

18 Herzog BA, Buechel RR, Husmann L, Pazhenkottil AP, Burger IA, Wolfrum M, *et al.* Validation of CT attenuation correction for high-speed myocardial perfusion imaging using a novel cadmium–zinc–telluride detector technique. *J Nucl Med* 2010; **51**:1539–1544.

19 Mouden M, Timmer JR, Ottervanger JP, Reiffers S, Oostdijk AH, Knollema S, Jager PL. Impact of a new ultrafast CZT SPECT camera for myocardial perfusion imaging: fewer equivocal results and lower radiation dose. *Eur J Nucl Med Mol Imaging* 2012; **39**:1048–1055.

20 Montemont G, Bordy T, Rebuffel V, Robert C, Verger L. CZT pixel detectors for improved SPECT imaging. Nuclear Science Symposium Conference Record; 19–25 October 2008; Dresden, Germany: NSS'08 IEEE; 2008.

21 Dvorak RA, Brown RK, Corbett JR. Interpretation of SPECT/CT myocardial perfusion images: common artifacts and quality control techniques. *Radiographics* 2011; **31**:2041–2057.

22 Shaw LJ, Berman DS, Maron DJ, Mancini GJ, Hayes SW, Hartigan PM, *et al.* COURAGE Investigators. Optimal medical therapy with or without percutaneous coronary intervention to reduce ischemic burden results from the Clinical Outcomes Utilizing Revascularization and Aggressive Drug Evaluation (COURAGE) trial nuclear substudy. *Circulation* 2008; **117**:1283–1291.

23 Slart RH, Tio RA, Zijlstra F, Dierckx RA. Diagnostic pathway of integrated SPECT/CT for coronary artery disease. *Eur J Nucl Med Mol Imaging* 2009; **36**:1829–1834.

24 Gould KL, Pan T, Loghin C, Johnson NP, Guha A, Sdringola S. Frequent diagnostic errors in cardiac PET/CT due to misregistration of CT attenuation and emission PET images: a definitive analysis of causes, consequences, and corrections. *J Nucl Med* 2007; **48**:1112–1121.

25 Berman DS, Abidov A, Kang X, Hayes SW, Friedman JD, Sciammarella MG, *et al.* Prognostic validation of a 17-segment score derived from a 20-segment score for myocardial perfusion SPECT interpretation. *J Nucl Cardiol* 2004; **11**:414–423.

26 Schinkel AF, Bax JJ, Delgado V, Poldermans D, Rahimtoola SH. Clinical relevance of hibernating myocardium in ischemic left ventricular dysfunction. *Am J Med* 2010; **123**:978–986.